

Full Paper

S.M.Sadat Kiai^{1*}, Mona Ghasemlou², S.H.Mahdian², A.Khalili^{1,2}

Conceptual study of ICP plasma as a thruster

¹Nuclear Science and Technology Research Institute (NSTR), Plasma and Nuclear Fusion Research School, A.E.O.I., 14155-1339 Tehran, (IRAN)
²Department of Physics and Institute for Plasma Research, Kharazmi University, 43, Dr. Mofatteh Avenue, 15719-14911, Tehran, (IRAN)

Received : April 07, 2015

Accepted : May 17, 2015

Published : May 27, 2015

*Corresponding author's Name & Add.

S.M.Sadat Kiai
Nuclear Science and Technology Research Institute (NSTR), Plasma and Nuclear Fusion Research School, A.E.O.I., 14155-1339 Tehran, (IRAN)

Abstract

The more plasma thrusters are employed in space usages, the more cost-effective they must be without losing device functionality. One of the most popular kinds of these plasma thrusters are Inductively Coupled Plasma (ICP) torches. They have a high performance and a distinctive operation in both efficiency and power-to-mass ratio. In this paper, an ICP plasma thruster operation is simulated under the atmospheric pressure by using MHD models and FlexPDE (Partial Differential Equation) software. Finally, having assumed steady state conditions, we have discretized linear equations. According to the initial and boundary conditions of the system, we have determined radial and axial velocity of the particles, the power dissipated, temperature, pressure, flow, flow driving force (thrust) as well specific impulse in each grid cell. To have a comprehensive study, the effect of the current source frequency and working gas flow rate on the thrust and specific impulse was investigated. Finally, some impurities in the working gas were implemented to find an optimized situation for the device.

Keywords

Inductively coupled plasma (ICP); Magneto-hydrodynamic model; Partial differential equation; Plasma thruster; Specific impulse.

INTRODUCTION

The name “Inductively Coupled Plasma” acronym (ICP) or plasma torch is a well-known apparatus and is nearly as old as the invention of electric power. The first report of an electrode-less ring discharge is given to Hittorf in 1884. The early effort to maintain ICP on a stream of gas could retrospect to Babat in 1947, and Reed in 1961^[1-2]. The history of ion propulsion engines, by accelerated charged particles thrown out of a chamber, generating driving force, goes back to the years 1906 to 1916. The idea of electric propulsion engines first was expressed by R. H. Goddard^[6-7].

There are two types of geometry for ICP: flat and cylindrical. In the form of a flat geometry, the spiral coil shaped electrode and in the cylindrical form the electrode is shape as a coil spring. The later type is

used as a plasma or ion engine. Conceptually, the induction plasma torch is extremely simple. Its essential components include a cylindrical refractory or quartz tube through which a working gas flows. A Radio Frequency (RF) power supply is coupling the energy to the plasma by means of helical coil of n turns surrounding the plasma tube and a means of initiating the discharge. The operating frequency supplied by RF generator is normally at $\sim 10 - 40$ MHz or even more. So, at such frequency the wavelength is about $\lambda \sim 30$ m which is much larger than the ICP dimension of the torch (few to tens of centimeters). In a sense, this means that the fields inside the ICP torch can be considered as static.

The cylindrical refractory or quartz tube consists of two concentric tubes which are separated by a distance of few millimeters. Around the outer tube is a spiral hollow copper coil, cooled by water and con-

finer the plasma inside the inner tube. The inner tube, the discharge gas inlet (usually argon or xenon) is converted into plasma and in the outer tube the inlet gas plays as a coolant. Charge carriers accelerated in the electric field (produced by RF current) couple their energy into the plasma via collisions with other particles. This collision induced ionization of the gas continues in a chain reaction, breaking down the gas into gas atoms, ions, and electrons, forming what are known as an ICP discharge.

Since 1960, inductively thermal plasma technology or inductively coupled plasma fuel is used in aerospace applications. In 1964 the first space vehicle using pulsed plasma propulsion was constructed^[4-9]. The first RF ion thruster was designed in 1960s: a 10-cm diameter of RF ion thruster, called the RIT-10, running at an ionization frequency of 1 MHz with a cylindrical ionization vessel using mercury for the propellant^[13-14]. The ICP torch propulsion engines are used for changing the speed and orbital elements of satellites.

The ion propulsion engines have lower fuel consumption, they are light, and have greater longevity, higher exit velocity gas and have a high specific impulse with the disadvantage of having limited thrust. However, it uses little power, and the desired speed can be achieved^[15-16]. A simplified schematic of the ICP plasma thruster is depicted in Figure 2. The objectives of this study are to simulate conceptual ICP plasma thruster and to find out the relationship between various parameters.

THEORETICAL METHOD

An inductively coupled plasma (ICP) is a type of plasma source in which the energy is supplied by electric currents originated from electromagnetic induction, that is, by time-varying magnetic fields. In cylindrical geometry, it is like a helical spring, when a time-varying electric current is passed through the coil, it creates a time-varying magnetic field around it, which in turn



Figure 1 : ICP torch; a) 40 MHz-2 KW, b) 13.56 MHz-1kW,^[10]

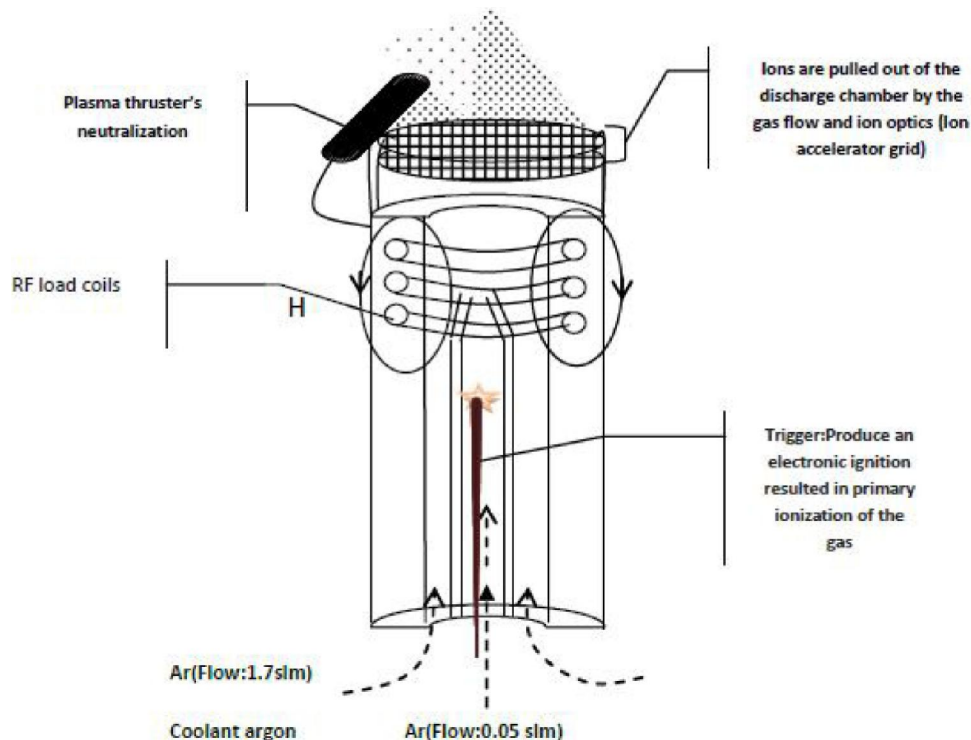


Figure 2 : A simplified schematic of the plasma thruster

induces azimuthally electric currents in the rarefied gas, leading to the formation of plasma. Argon is one example of a commonly used rarefied gas. Plasma temperatures inside the inner tube can reach ~ 10000 K, comparable to the surface of the sun. The ICP discharges are of relatively high electron density, on the order of $\sim 10^{15}$ cm⁻³. As a result, ICP discharges have wide applications where high-density plasma is needed^[11-12].

When an RF generator is on, the magnetic flux is produced by helical current that penetrates into the adjacent tube discharge region. According to the Faraday's law of induction, the time varying magnetic flux \vec{B} induces a solenoidal time varying electric field \vec{E} . It is the inductive electric field which then accelerates free electrons in the discharge and sustains the plasma^[3]. The electromagnetic behavior of the induction plasma, described by Maxwell's equations, is very complicated. Maxwell's equations consist of a set of coupled first-order partial differential equations, which are obtained from Gauss' law, Coulomb's law, Faraday's law and Ampere's law and relating the various components of the electric and magnetic fields. Therefore, the first step is to solve Eq.1 (see below) to obtain electromagnetic behavior of induction plasma. Since the vector potential \vec{A} is parallel to the applied current density \vec{j} , it has two azimuthal and axial components: $= A_\phi + A_z$ ^[3]. Once we have found solutions for A_ϕ and A_z in appropriate boundary conditions, the field components E_ϕ , E_z and H_r , H_ϕ , H_z are obtained. Since the applied current is assumed to be sinusoidal with RF, it is reasonable to expect that the induced fields \vec{E} , and \vec{H} and vector potential \vec{A} are also sinusoidal^[3].

Magneto-hydrodynamics describes the physical behavior of inductively coupled plasma. Properties normally ascribed to fluids include density, compressibility, and viscosity. In cylindrical coordinates, three velocity components (i.e. radial $v_r(r, z)$, tangential $v_\phi(r, z)$ and axial $v_z(r, z)$) represent the flow of the gas. In three dimensional axi-symmetric forms, the corresponding momentum equations are given in Eq.5 (see below). Momentum equations described in Eq.5 are also called Navier-Stokes equations. The energy equation, Eq.6 (see below), has to be solved to obtain the temperature value in all parts of the torch area^[3]. It has been noticed that since the number of particles is very large and the Personal Computer (PC) memory is limited, the equation for the current has given the following parameters; flowing argon 0.05 liter per minute for rocket fuel, flow flowing argon gas at 1.7 liters per minute as cooling system, frequency source 18.84 MHz

and acceleration voltage of 100 volts. Initially the temperature at each grid cell determined by the vector potential and the electric field and thus, propulsion and specific impulse could be obtained. This process is repeated until the plasma is formed and the flame is out of ICP torch.

It takes about One hour to solve these equations by the computer with AMD X4 945 Processor and reach the desired results. Simulated model permits to predict RF coil current, frequency, plasma power, overall efficiency of the generator. All RF plasma thrusters subsequently designed followed these basic design principles. This model can be useful as a design tool for the induction plasma generator. The followings are the governing equations for ICP torch.

With the help of the preceding discussion, electromagnetic behavior of the standard induction plasma is described by two components of the vector potential; A_ϕ , due to circular contribution of the applied current and A_z is due to the axial contribution of applied current^[3]. From Maxwell equations we have:

$$\nabla^2 \vec{A} = i\mu_0 \omega \sigma \vec{A} \quad (1)$$

After separating azimuthal and axial components and dividing them into real and imaginary parts, the final equations will be:

$$\nabla^2 \text{Re}(A_\phi) - \frac{\text{Re}(A_\phi)}{r^2} + \mu_0 \omega \sigma \text{Im}(A_\phi) = 0$$

$$\nabla^2 \text{Im}(A_\phi) - \frac{\text{Im}(A_\phi)}{r^2} - \mu_0 \omega \sigma \text{Re}(A_\phi) = 0$$

$$\nabla^2 \text{Re}(A_z) + \mu_0 \omega \sigma \text{Im}(A_z) = 0$$

$$\nabla^2 \text{Im}(A_z) - \mu_0 \omega \sigma \text{Re}(A_z) = 0$$

Once the vector potential is obtained, other electromagnetic parameters can be calculated. The electric field:

$$\vec{E}_\phi = -i\omega A_\phi \quad (2)$$

$$\vec{E}_z = -i\omega A_z \quad (3)$$

and the magnetic field:

$$\vec{B} = \vec{\nabla} \times \vec{A} \rightarrow \begin{cases} H_r = \frac{1}{\mu_0} \left(\frac{\partial A_z}{r \partial \phi} - \frac{\partial A_\phi}{\partial z} \right) \\ H_\phi = -\frac{1}{\mu_0} \left(\frac{\partial A_z}{\partial r} \right) \\ H_z = \frac{1}{r\mu_0} \left(\frac{\partial(rA_\phi)}{\partial r} \right) \end{cases} \quad (4)$$

Note that the radial component of vector potential A_r is omitted because of the applied current density. Here, we present momentum equations describing ICP torch particle velocity (Navier-Stokes equations). To derive

these equations, one has to use the continuity equation and do some mathematical operations to achieve the following equations:

$$\rho \frac{\partial v_r}{\partial t} + \rho \vec{v} \cdot \nabla v_r - \rho \frac{v_r^2}{r} = -\frac{\partial P}{\partial r} + F_r + \vec{\nabla} \cdot (\mu \vec{\nabla} v_r) + \vec{\nabla} \cdot \left(\mu \frac{\partial \vec{v}}{\partial r} \right) - \frac{\mu v_r}{r^2} \quad (5)$$

$$\rho \frac{\partial v_\phi}{\partial t} + \rho \vec{v} \cdot \nabla v_\phi + \rho \frac{v_r v_\phi}{r} = F_\phi + \vec{\nabla} \cdot (\mu \vec{\nabla} v_\phi) - \frac{\mu v_r}{r^2} - \frac{v_\phi}{r} \frac{\partial \mu}{\partial r}$$

$$\rho \frac{\partial v_z}{\partial t} + \rho \vec{v} \cdot \nabla v_z = -\frac{\partial P}{\partial z} + F_z + \vec{\nabla} \cdot (\mu \vec{\nabla} v_z) + \vec{\nabla} \cdot \left(\mu \frac{\partial \vec{v}}{\partial z} \right)$$

where $\vec{\nabla} = \frac{\partial}{\partial r} \hat{r} + \frac{\partial}{\partial z} \hat{z}$, \square dependency is ignored in 2D due to axi-symmetry, ρ is the gas density, t is the time, P is the pressure, μ is the viscosity and F_r, F_ϕ, F_z are components of Lorentz force^[3].

Lorentz force, \vec{F} :

$$F_r = +\frac{1}{2} \sigma \mu_0 Re \{ E_\phi H_z^* - E_z H_\phi^* \} \quad (6)$$

$$F_\phi = +\frac{1}{2} \sigma \mu_0 Re \{ E_z H_r^* \}$$

$$F_z = -\frac{1}{2} \sigma \mu_0 Re \{ E_\phi H_r^* \}$$

We can also write the following relation (energy equation) for the plasma temperature:

$$\rho c_p \frac{dT}{dt} = \nabla_k (k \nabla_k T) + \sigma_{ik} \nabla_k v_i + \frac{1}{2} \sigma Re (E_i \cdot E_i^*) \quad (7)$$

Here, k is the thermal conductivity, c_p is the heat capacity, T is the temperature, and E_i is component of the electric field. All values for: ρ, C_p, μ, σ and k are taken from the report by Miller and Ayen^[18]. Equations (1)-(7) are coupled differential equations with partial derivatives which need to be solved numerically and simultaneously with the proper initial and boundary conditions. This is done by the commercial version of FlexPDE5 software.

For the thrust and specific impulse

$$T = \dot{m} u_e \quad (8)$$

$$I_{sp} = \frac{\dot{m} u_e}{m g} \quad (9)$$

Where: T is thrust, \dot{m} is Propellant mass flow rate, I_{sp} is specific impulse, u_e is velocity of the rocket exhaust particles, and g is gravity in space (the earth's gravity divided by 1000 is equal to space gravity).

Figure 3 shows the applied forces found in two-grid accelerator systems. The thrust, which is the force supplied by the ICP torch to the spacecraft, is equal to the sum of the forces on the screen and accelerating grids. This net force, Eq. 10, on the grids is equal to and opposite from the electrostatic forces, ion on an ion between the grids.

$$F_{ion} = \frac{1}{2} \epsilon_0 (E_{accel}^2 - E_{screen}^2) \quad (10)$$

where ϵ_0 is the electric permittivity of free space, E_{accel} is the electric field at the acceleration grid and E_{screen} is the electric field at the acceleration grid and E_{screen} is the electric field at the screen^[13]. The distance between the accelerator grid is taken to be 10^{-3} m and the potential difference 100 V.

Also, the mass flow output from the rocket can be written as;

$$\dot{m} = \frac{AP_t}{\sqrt{T_t}} \sqrt{\frac{\gamma}{R}} \left(\frac{\gamma + 1}{2} \right)^{-\frac{\gamma+1}{2(\gamma-1)}} \quad (11)$$

where R ($8.314472 \text{ J} \cdot \text{K}^{-1}$) is the gas constant; γ (1.66) heat capacity ratio; and A (2.5mm) is the area accelerator page; T_t is the final temperature of the gas, P_t is the final pressure of the gas, P_t is the final pressure of the gas^[17]. Equations (8)-(11) are also solved during the calculations. The obtained results will be discussed next.

RESULTS AND DISCUSSION

The corresponding governing Equations (1)-(11) are solved numerically by applying a Finite Element Method (FEM) with Partial Differential Equation solver (Flex PDE5). Based on Magneto-hydrodynamics model (describes the physical behavior of inductively coupled plasma) the plasma behavior and its

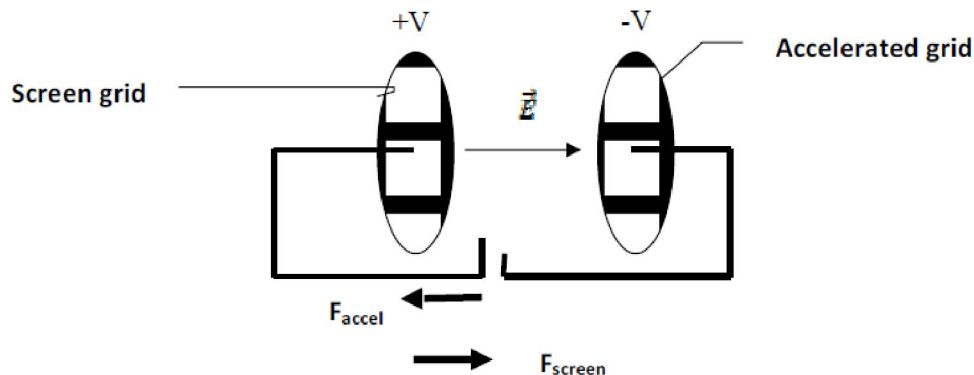


Figure 3 : Forces on a two-grid acceleration system

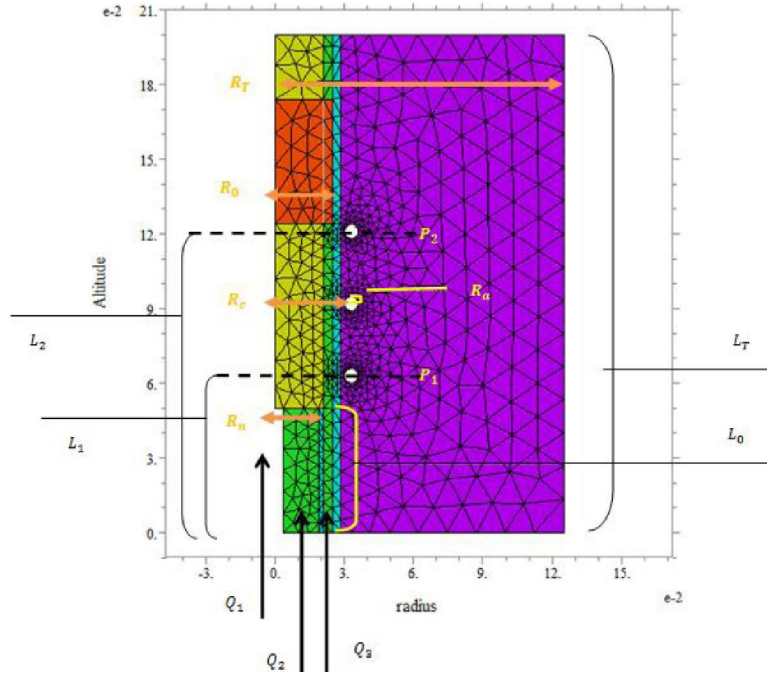


Figure 4 : Torch geometry; RF current is applied to two ends P_1 and P_2 . Argon gas flows into the inlet region of the torch tube with different flow rates Q_1 , Q_2 , and Q_3 . Plasma is generated in the coil region with radius R_n which is less than R_0 .

TABLE 1 : Plasma torch dimensions and operation conditions (slpm: standard liter per minute)

$Q_1 = 1.0$ slpm	$R_m = 3.7$ mm	$L_0 = 50$ mm
$Q_2 = 0.05$ slpm	$R_n = 18.8$ mm	$L_1 = 63$ mm
$Q_3 = 1.7$ slpm	$R_0 = 25$ mm	$L_2 = 121$ mm
$I_{coil} = 200$ A	$R_c = 33$ mm	$L_T = 200$ mm
$R_a = 3$ mm	$R_T = 100$ mm	$\delta_w = 3.5$ mm

properties are examined in terms of plasma parameters. The ICP torch geometry considered in the present work is shown in Figure 4. The governing Equations with the prescribed boundaries and initial conditions are solved using parameters listed in TABLE (1).

The calculations were performed for about 2825 nodes and 1359 cells in non-uniform grid system and the time it took to run the program was about an hour.

The maximum real vector potential is close to the coils according to the induced currents flowing skin depth and the skin depth near the coil. This area is a maximum real vector potential (the coil current density is proportional to the vector potential). Imaginary vector potential has a maximum value at the center of the torch. This component represents an area of potential sources of radio frequency energy absorption and dissipation of the plasma torch; because skin depth field in central ICP torch tube damped RF currents and this region is the most absorbing and dissipating energy. The maximum temperature at torch outlet is 32100 K. The actual thrust is at the edge of the end of ICP torch, just because of the speed and the maximum axial thrust force, which is proportional to the

speed of axial output of torch nozzle. If we increase the frequency of the source, then the thrust and specific impulse increases, but because the skin depth decreases as we increase the frequency (13.56 MHz maximum frequency is the skin depth), there must be a limit.

R_0 is the radius of the outer cylinder, R_m for spectroscopy, R_n is radius of the inner cylinder, R_c is the outer radius of the coil, R_a is the inner radius of the coil, L_0 the height of the inner cylinder, L_1 the starting point of the coil winding, L_2 the coil end point winding, L_T the height above torch nozzle.

The value of the thrust as a function of RF frequency is depicted in Figure (5). As can be seen, driving force increases with increasing frequency source, since the

thrust is proportional to the ratio $\frac{P}{\sqrt{T}}$ and this ratio increases with increasing frequency. But it can be deduced that the thrust reaches to a saturation level beyond the 8 MHz frequency. Also, the effect of gas flow rate on the thrust at 3 MHz frequency is shown in Figure (6). In figure (5) variations of thrust with the frequency after 3 MHz is not significant. In figure (6) variations of thrust with the flow rate MHz is not significant between 8 to 12 slpm.

Figure (7) represents specific impulse as a function of frequency. As can be seen on the figure, specific impulse depends on the applied RF frequency; having frequency increased, plasma resistance increases due to the temperature raise, and thus the output velocity

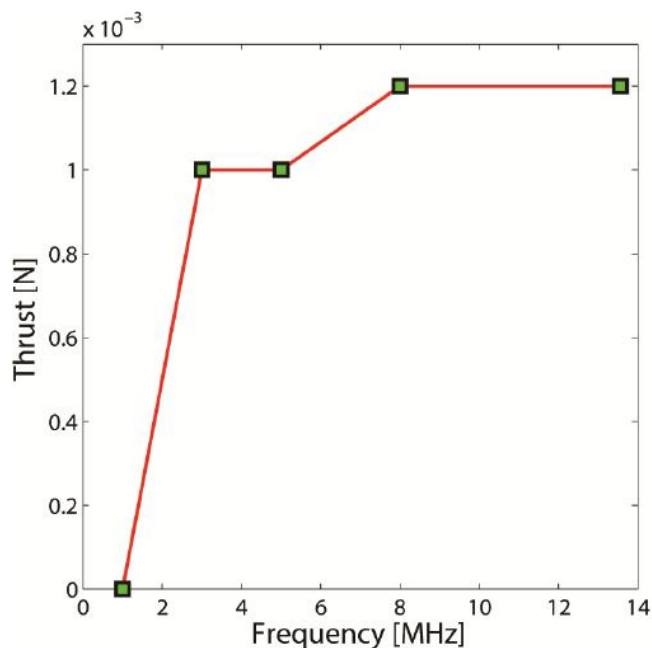


Figure 5 : The variation of the thrust as function of frequency

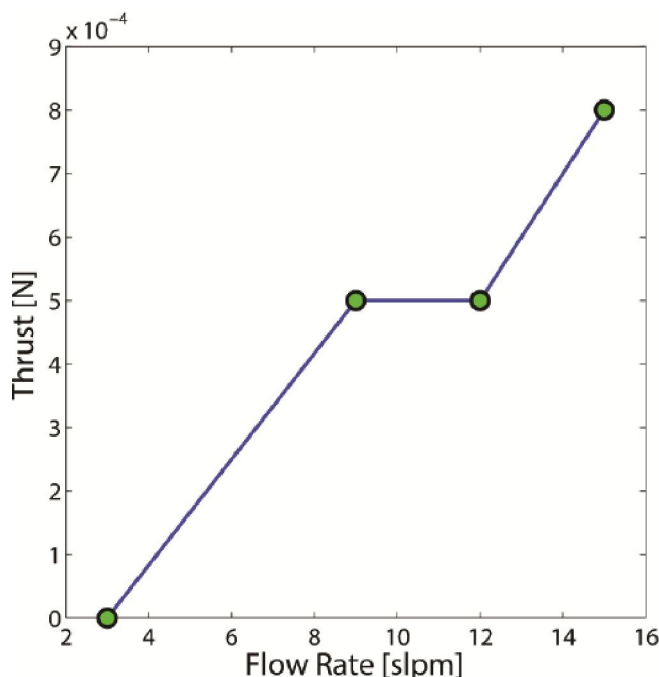


Figure 6 : The variation of the thrust with gas flow rate at 3 MHz

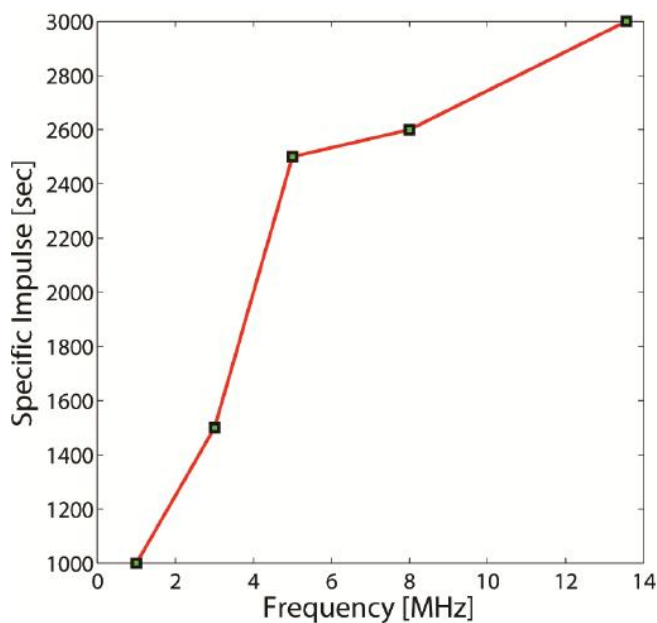


Figure 7 : Variation of the specific impulse versus frequency

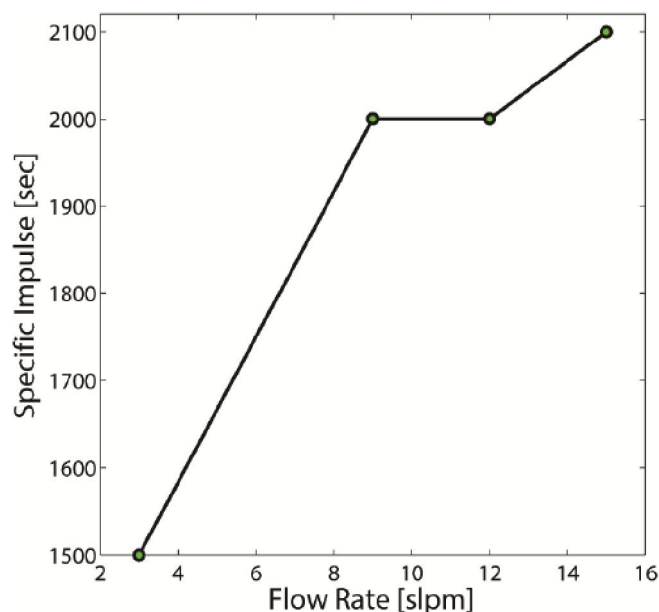


Figure 8 : Variation of the specific impulse with gas flow rate at 3 MHz

of the particles increases as a result of increased specific impulse. Figure (8) shows the variation of the specific impulse at 3 MHz when the gas flow rate increases. In Figure (9) we have shown the driving force in two dimensions. As shown in this figure, thrust force is so small inside the plasma region and approximately zero in some points. This result is close to the desired goal. In Figure (10), the specific impulse at 13.56 MHz is shown. Maximum value of the specific impulse is found to be 2500 s near the outlet of the torch but mostly is about 2000 s in this area.

To study the effect of working gas on these two parameters, some admixtures with small percentages were added to the pure Argon gas theoretically. During the

calculation process, %0.1 Helium, %0.5 Helium, %0.5 Krypton, %1.0 Krypton and %0.5 Xenon were added to the pure Argon gas and the results are compared in Figures (11) and (12). Methods for gas mixing to calculate the transport coefficients are described and provided by *A. B. Murphy*^[19]. As shown in Figure (11), the thrust force doesn't vary by adding %0.1 Helium to the working gas at 3 MHz frequency but at 5 MHz shows a small change. Adding %0.5 Helium or %0.5 Krypton increases the thrust force but %0.5 Xenon makes it approximately close to zero. This is due to the greater atomic mass of additives compared with

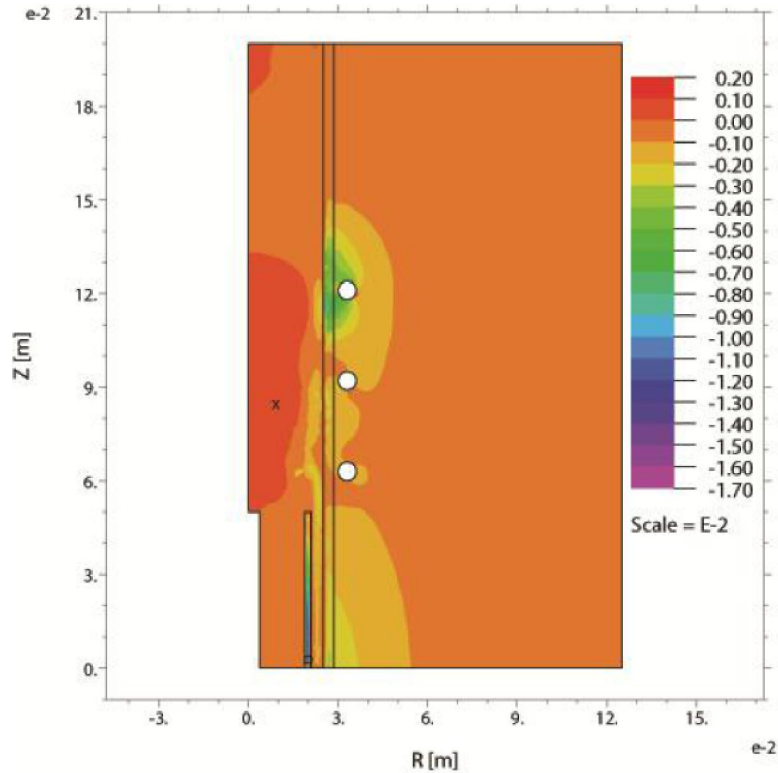


Figure 9 : The propulsion force or thrust at 13.56 MHz (N)

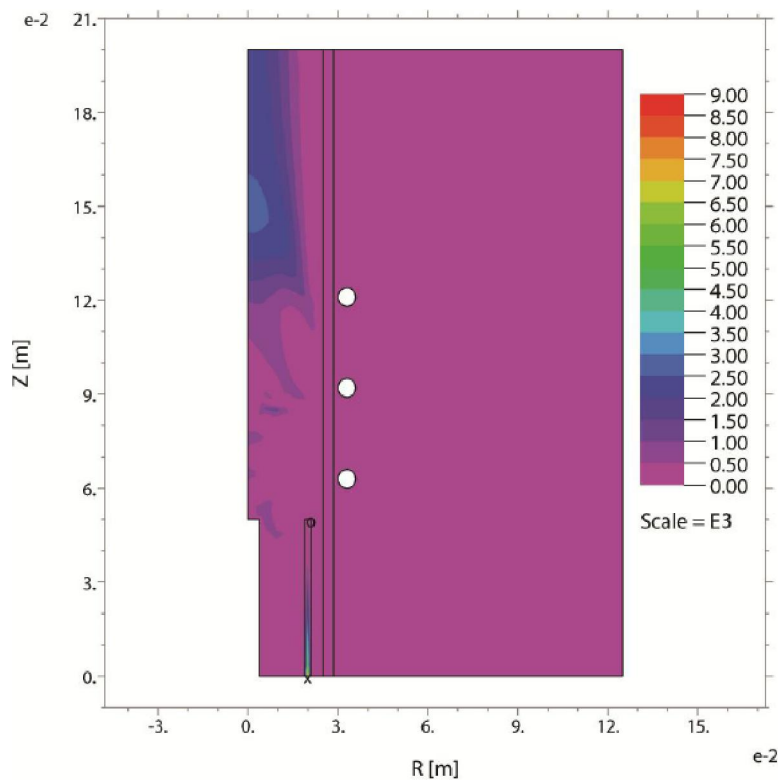


Figure 10 : Specific Impulse at 13.56 MHz (sec)

the Argon's. Figure (12) shows a significant increase in specific impulse while %0.1 Helium was added both for 3 and 5 MHz and reaches 3000 and 4000 s respectively which is a remarkable improvement. For cases %0.5 Helium, %0.5 and %1.0 Krypton, the specific impulse has a significant increase about 500 and 1500 s

at 3 MHz and about 1000 and 1500 s at 5 MHz compared the pure Argon case. At 3 MHz, the specific impulse decreases to 500 sec by adding %0.5 Xenon while at 5 MHz enhances up to 2500 sec which is adjustable with the atomic mass and frequency relation.

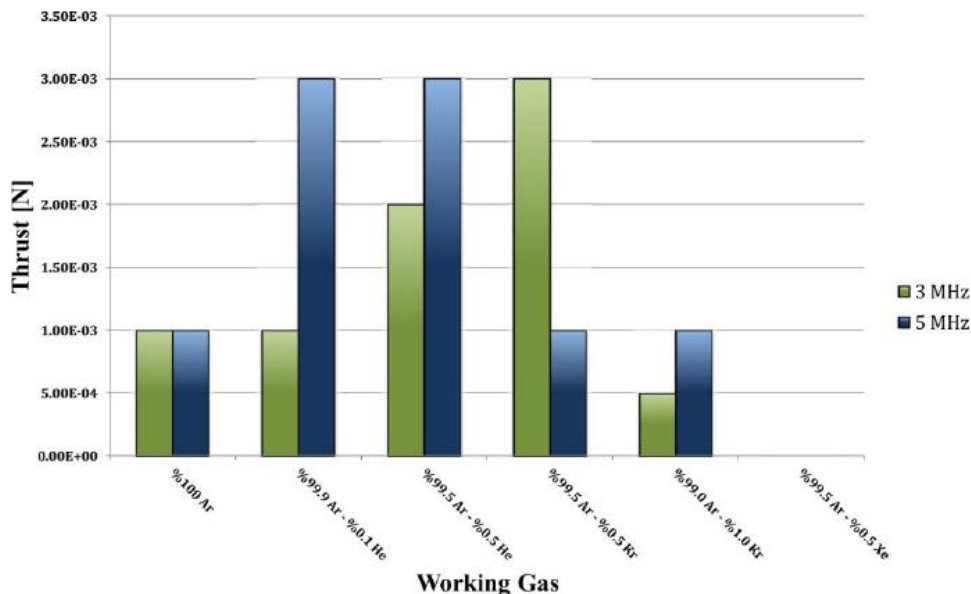


Figure 11 : Comparing the Thrust force (N) in pure Argon with other admixtures running at 3 and 5 MHz (values have been selected to the last digit)

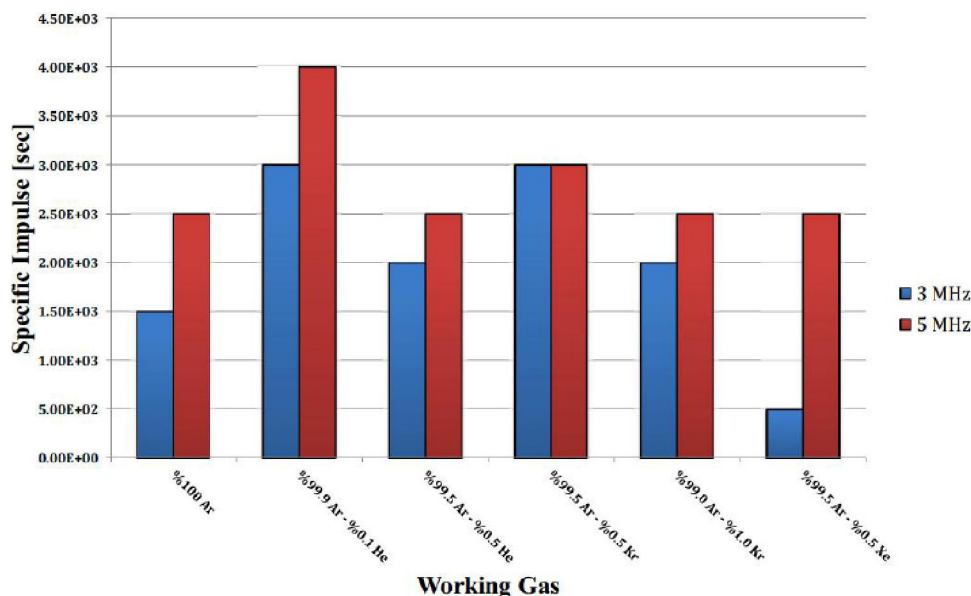


Figure 12 : Comparing the Specific Impulse (sec) in pure Argon with other admixtures running at 3 and 5 MHz (values have been selected to the last digit)

CONCLUSION

The acceleration of space’s gravity is about 1000 times smaller than the acceleration of Earth’s gravity. Thus, such an ion engine is appropriate for the deviations of satellite orbits. By increasing the RF frequency source, employing the accelerator grid and increasing the gas flow rate, one can get higher Specific Impulse, thereby; this will increase the lifetime of the spacecraft and plasma thruster engine efficiency. Adding some impurities with specific and proper percentages can help us to improve the device’s performance. However, the device performances could be optimized by adding gas admixture rocket fuel such as potassium in xenon, to create a better output plasma energy beam with lower

current consumption.

ACKNOWLEDGMENT

The authors would like to gratefully and sincerely thank *Dr. Murphy* from *CSIRO Materials Science and Engineering* for his cooperation and providing the data needed for calculations.

REFERENCES

- [1] G.1.Babat; last.Elec.Eng., Londen Eng., 94, 27 (1947).
- [2] T.B.Reed; J.Appl.Pbys., 32, 821 (1961).
- [3] Modeling of helically applied current to the inductively coupled radio frequency plasma torch in two

- dimensions, A thesis submitted to the graduate school of natural and applied sciences of the Middle East technical university by mehmet canturk, department physics, January, (2004).
- [4] R.H.Goddard; An autobiography, Robert H.Goddard Notebook dated September 6 1906, astronautics, and book, Ion propulsion for space flight-ERNST STUHLINGER, 4, 24, (1959).
- [5] NASA Facts, National aeronautics and space administration, Glenn Research Center, Cleveland, Ohio 44135-3191, FS-2004-11-023-GRC.
- [6] Mark Wright; April 6, Science Nasa.Gov., Ion Propulsion 50 years in the making, (1999).
- [7] H.Robert, Goddard, American Rocket Pioneer; Smithsonian Scrapbook, Smithsonian Institution Archives, Retrieved 28 March, (2012).
- [8] Ann Arbor; The 31 st international electric propulsion conference, University of Michigan, USA September 20 – 24, (2009); Hideo Sugai, Kenji Nakamura, Keiji Suzuki; “Electrostatic coupling of antenna and the shielding effect in inductive RF Plasma”, Jpn.J.Appl.Phys., 33-4B, 2189-2193 (1994); K.Suzuki, K.Nakamura, H.Ohkubo, H.Sugai; “Power transfer efficiency and mode jump in an inductive RF discharge,” Plasma Sources Sci.Technol., 7, 12-20 (1998).
- [9] State-space modeling of the radio frequency inductively-coupled plasma generator Rakesh Kumar Dewangan, Sangeeta B Punjabi, N.K.Joshi, D.N.Barve, H.A.Mangalvedekar, B.K.Lande.
- [10] Nuclear science and technology research institute (NSTR), Plasma and nuclear fusion research school, Plasma engine system Lab, A.E.O.I., 14155-1339 Tehran-Iran.
- [11] Rakesh Kumar Dewangan *et al.*; *J.Phys., Conf.Ser.*, 208 012056. doi:10.1088/1742-6596/208/1/012056, (2010).
- [12] A.Montaser, D.W.Golightly; eds.Inductively Coupled Plasmas in Analytical Atomic Spectrometry, VCH Publishers, Inc., New York, (1992).
- [13] D.H.Goebel, I.Katz; Fundamentals of electric propulsion: Ion and hall thrusters, JPL Space Science and Technology Series, http://meyweb.physik.uni-giessen.de/rit/bilder/rits/big/rit10_hg1.jpg, (2008).
- [14] A dissertation in electrical engineering by valerie F.M.Mistoco, Modeling of small scale radio-frequency inductive discharges for electric propulsion applications, Submitted in partial fulfillment of the requirements for the degree of doctor of philosophy, August, (2011).
- [15] Choueiri, Y.Edgar; New dawn of electric rocket *Scientific American*, doi:10.1038/scientific American, 0209-58, 300, 58-65 (2009).
- [16] Electric versus chemical propulsion, *Electric Spacecraft Propulsion*, ESA. Retrieved 17th February, (2007).
- [17] <http://www.grc.nasa.gov/WWW/k-12/airplane/rktthsum.html>
- [18] C.Reid, Miller; Richard J.Ayen, J.Appl.Phys., doi: 10.1063/1.1657382, 40, 5260 (1969).
- [19] A.B.Murphy; ‘Transport coefficients of helium and argon-helium plasmas’, *IEEE Trans.Plasma Sci.*, 25, 809-814 (1997).